Thin-Walled Structures 56 (2012) 1–8

Contents lists available at SciVerse ScienceDirect

Thin-Walled Structures

journal homepage: www.elsevier.com/locate/tws

Structural-acoustic aspects in the modeling of sandwich structures and computation of equivalent elasticity parameters

Ryan L. Harne, Clement Blanc, Marcel C. Remillieux *, Ricardo A. Burdisso

Department of Mechanical Engineering, Virginia Tech, 149 Durham Hall (MC 0238), Blacksburg, VA 24061, USA

ARTICLE INFO

Article history:
Received 15 December 2011
Received in revised form
3 March 2012
Accepted 15 March 2012
Available online 5 April 2012

Keywords:
Sandwich structures
Small-deflection theory
Equivalent stiffnesses
Discrete connections
Fluid–structure interaction

ABSTRACT

Small-deflection theory is used along with FE models to compute the equivalent elasticity parameters of sandwich structures. Eigenfrequency and eigenmode analyses, comparing the equivalent 2-D continua with full 3-D models, are utilized to determine how continuous connections and in-vacuo assumptions are influenced as real-world discontinuities and gas- or foam-filled cavities are included. It is found that discrete connections between structural elements reduce stiffnesses and eigenfrequencies of the net structure substantially. The presence of gas or foam in the core cavities is observed to increase the overall damping of the dynamic panel response while also amplifying certain panel resonances.

1. Introduction

Typically, structural-acoustic problems are solved by implementing a mathematical model of the structure exhibiting dynamics of reduced complexity. Equivalent elasticity parameters play an important role in this regard by providing the researcher with materials or structures having nearly identical static and dynamic characteristics as the original complex specimen. For instance, in the field of building construction and analysis, such approach is commonly followed in the study of structural response to seismic excitation [1–3].

Residential buildings in the United States are made primarily of stud-framed walls, which consist essentially of stiffeners sandwiched between plaster and wood (e.g., oriented strand board) panels, with insulation materials (e.g., fiberglass wool) filling the cavities. Sandwich panels are also used extensively in industrial buildings but the facing and core elements typically consist of thin-walled, cold-formed steel sheets and rigid foamed insulation, respectively. A comprehensive structural analysis has been carried out by Chong and Hartsock [4] for this type of structure, including the mechanisms of flexural stresses, deflections, vibration, and thermal stresses, thus summarizing two decades of research on the topic. Stiffened plates differ from uniform plates in that their properties are directional, i.e., their bending rigidity about one axis is not necessarily the same as the bending rigidity about a perpendicular axis. The computational effort can be reduced dramatically by modeling a stiffened wall as an equivalent homogeneous orthotropic 2-D continuum. This simplification is usually valid at low frequencies, i.e., when the bending wavelength is larger than the distance between the wall stiffeners. At higher frequencies, the wall components (e.g., panels, studs, and insulation material) have to be modeled separately and cannot be smeared into an equivalent uniform material.

A considerable amount of work has been devoted to modeling, analyzing, and designing thin-walled sandwich structures with core layers having truss, sinusoidal, honeycomb, and otherwise periodic cross sectional geometries. A comprehensive review on this topic was provided by Noor and Burton [5]. Mainly two approaches may be considered to compute the equivalent properties of sandwich structures. In the first approach, which is used in this paper, the core layer is modeled as an equivalent continuum and is then combined with a plate model. In the plate model, the sandwich structure is modeled as several layers with approximations made in the direction of the thickness. Analytical expressions for the characteristics of the equivalent continuum are derived from a strength-of-materials type of theory [6,7]. A more recent approach is based on the homogenization theory, which is essentially an asymptotic expansion method taking benefit from the periodicity of the structure. In this approach, two small parameters are defined: e, the ratio of the panel thickness to characteristic length of the panel and ε, the ratio of one period length of the panel to the characteristic length of the panel. The

* Corresponding author.
E-mail addresses: rharne@vt.edu (R.L. Harne), cblanc@vt.edu (C. Blanc), mremilli@vt.edu (M.C. Remillieux), rburdiss@vt.edu (R.A. Burdisso).

0263-8231/$ - see front matter © 2012 Elsevier Ltd. All rights reserved.
http://dx.doi.org/10.1016/j.tws.2012.03.012

original heterogeneous specimen is then modeled as an equivalent homogeneous plate by making these two small parameters tend to zeros. Several homogenization approaches exist, based on the order in which these parameters tend to zero (e.g., both simultaneously or one after the other). More details on the homogenization techniques may be found in the book of Lewinski and Telega [8] as well as in references [9,10].

Most studies implicitly utilize in-vacuo conditions for the cavities enclosed by the sandwich structure and also assume that the periodic core geometry contacts the facing sheets continuously. These conditions are rarely met in practice. For instance, in building construction, nails are used to hold the studs to the wood or plaster panels and wall cavities are filled with insulation materials. Therefore, there is a need to understand how the vibration response of sandwich structures is affected by air-filled or foam-filled cavities and how the computation of equivalent elasticity parameters for continuous connections between the core and facing sheets compares to that for punctual (discrete) connections. Recently, Burlayenko and Sadowski [11] studied the effect of foam-filled cavities on the free vibration and buckling characteristics of a honeycomb sandwich structure. They found that foam had little influence on the mode shapes of the structure. However, their work was limited to the first two modes of vibration of the structure and lacked an analysis of the effect of foam on the dynamic response.

This paper is organized as follows. Section 2 describes the approach followed to compute equivalent elasticity parameters of three-layered sandwich structures. Finite element (FE) analysis is utilized for this purpose. An example case is then studied. Natural frequencies and mode shapes of a 2-D Mindlin plate with equivalent elastic constants are compared to those of a 3-D shell structure to validate the approach. Section 3 investigates the effect of discrete connections between the core and facing elements on the equivalent elasticity parameters and on the resulting eigenproperties. Section 4 studies the effects of air- and foam-filled cavities on the vibration response of a sandwich structure to determine how such an inclusion would modify the usefulness of the FE approach. It is shown that elastic homogenization techniques are easily applicable to realistic building construction scenarios, provided attention is given to the relative inertial and damping influence of the embedded gas or elastic material (e.g., foam) within the cavities of the sandwich structure. Section 5 reports the main conclusions of this study.

2. Small deflection theory

2.1. Methodology

Libove and Batdorf [6] derived a model for the determination of equivalent elastic properties for incompressible sandwich panels having an arbitrary core design. This method transforms the exact core geometry into an equivalent homogeneous orthotropic 2-D continuum, having bending, twisting and shearing stiffnesses D_x, D_y, D_{xy}, D_{Qx}, and D_{Qy}, respectively. Included with the derivation were a series of experiments which may be implemented with manufactured specimen panels to determine the elasticity constants. Cheng et al. [12] then proposed and validated a set of corresponding FE models to expedite the computation of such elastic properties. The latter FE models are employed here to evaluate the equivalent bending and twisting stiffnesses of the panels. To determine equivalent shearing stiffness characteristics, the three-point bending test carried out with FE models described by Nordstrand et al. [7] and based on ASTM standard C393-62 is utilized.

2.1.1. Force-distortion governing equations

The exact geometry of the periodic sandwich panel under study is shown in Fig. 1(a). The distortion equations for the incompressible sandwich panel are [6]:

$$\kappa_x = \frac{\partial^2 w}{\partial x^2} = -\frac{M_x}{D_x} + \frac{\nu_y M_y}{D_y} + \frac{1}{D_{Qx}}\frac{\partial Q_x}{\partial x} \tag{1}$$

$$\kappa_y = \frac{\partial^2 w}{\partial y^2} = -\frac{M_y}{D_y} + \frac{\nu_x M_x}{D_x} + \frac{1}{D_{Qy}}\frac{\partial Q_y}{\partial y} \tag{2}$$

$$\kappa_{xy} = \frac{\partial^2 w}{\partial x \partial y} = \frac{M_{xy}}{D_{xy}} + \tfrac{1}{2}\frac{1}{D_{Qx}}\frac{\partial Q_x}{\partial y} + \frac{1}{2}\frac{1}{D_{Qy}}\frac{\partial Q_y}{\partial x} \tag{3}$$

where M_x and M_y are internal bending moments, M_{xy} is the internal twisting moment, Q_x and Q_y are internal shearing forces, and ν_x and ν_y are the Poisson's ratios coupling the bending responses. These moments and forces are labeled for a unit core cross-section in Fig. 1(b) having thickness h_f and period $2p$. The curvatures and twist, κ_x, κ_y, and κ_{xy}, are defined about the middle-plane of the panel.

The facing sheets and the core layer are considered to be isotropic materials of thicknesses t_f and t_c, respectively. The FE models to calculate the equivalent stiffnesses for the sandwich structure (i) define a 3-D geometry of a certain section of the sandwich core; (ii) apply the loads described in the distortion equations; and (iii) calculate the resulting strains or displacements from key nodes. Likewise with careful undertaking of the described laboratory tests [6], the FE models allow one to immediately apply the desired moments and/or shearing forces such that it is assumed the remaining moments and forces in Eqs. (1)–(3) are zero. For instance, in Eq. (1), the bending moment M_x is applied in the FE model but no moment M_y or shear Q_x are applied and thus the equation is reduced to $\kappa_x = -M_x/D_x$.

The FE models to compute these equivalent elastic constants E_x, E_y, G_{xy}, ν_x, and ν_y are depicted in Fig. 2. These are only schematics of the FE model geometries and do not represent meshed versions of the models. The model to compute E_x uses geometries of a single core period, $2p$, with a length of sufficient span so as to ignore end effects. Increasing this length naturally reduces the influence of potential end effects on the deformation at the center of the specimen, but becomes more costly to compute due to the increasing number of finite elements. The model to calculate E_y uses multiple periods of the sandwich structure and a depth equal to or greater than the period length.

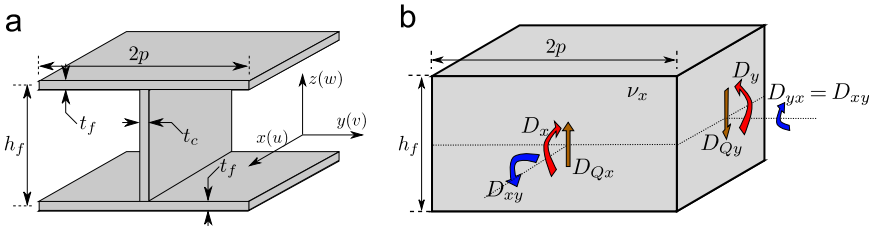

Fig. 1. (a) Exact geometry of sandwich panel having period $2p$. (b) Equivalent continuous material having bending, twisting and shearing stiffnesses D_x, D_y, D_{xy}, D_{Qx}, and D_{Qy}.

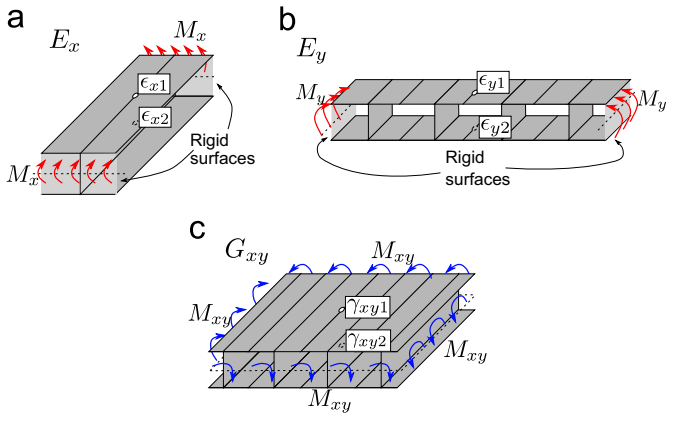

Fig. 2. (a) FE model to compute equivalent E_x elasticity parameter of sandwich panel. (b) FE model to compute E_y. (c) FE model to compute G_{xy}. Each model indicates centrally-located nodes and the output parameters required to be extracted at these locations.

The model to calculate the twisting stiffness, G_{xy}, uses a geometry of equal length and depth.

Unit moments per area are applied to rigid end elements in the models to compute bending stiffnesses, as shown in Fig. 2 (a) and (b). Rigid elements are modeled by using a Young's modulus six orders of magnitude greater than the facing sheet value. For the twisting stiffness model, Fig. 2(c), unit moments are applied without rigid end planes, since additional rigidity would inhibit the sample deflection. In each model, sides of the geometry to which no moments or forces are applied are given boundary conditions of symmetry. This implies that displacements in the co-ordinate axis normal to the plane of symmetry must be zero.

In Fig. 2, the desired output quantities of each model are provided in inset boxes. Bending strains and shearing strains are appropriately output at centrally positioned nodes on the top and bottom facing sheets for the models to compute bending and twisting stiffnesses, respectively. Using the strains, the bending and twisting curvatures are calculated as follows [12],

$$\kappa_x = \frac{\varepsilon_{x1}-\varepsilon_{x2}}{h_f}, \quad \kappa_y = \frac{\varepsilon_{y1}-\varepsilon_{y2}}{h_f}, \quad \kappa_{xy} = \frac{\gamma_{xy1}-\gamma_{xy2}}{2h_f} \tag{4}$$

These parameters relate to the bending stiffnesses, shear stiffnesses, and Poisson's ratios as,

$$D_x = -\frac{M_x}{\kappa_x}, \quad D_y = -\frac{M_y}{\kappa_y}, \quad D_{xy} = \frac{M_{xy}}{\kappa_{xy}} \tag{5}$$

$$\nu_x = \frac{\kappa_y}{M_x/D_x}, \quad \frac{\nu_x}{D_x} = \frac{\nu_y}{D_y} \tag{6}$$

Since unit moments per area were employed in the FE models, the stiffnesses given in Eq. (5) are straightforward to calculate. From the computed stiffnesses may be found the equivalent elastic material properties representing a 2-D incompressible, homogeneous orthotropic plate,

$$E_x = \frac{12D_x}{h_f^3}, \quad E_y = \frac{12D_y}{h_f^3}, \quad G_{xy} = \frac{6D_{xy}}{h_f^3}, \quad \nu_{yx} = \nu_y \tag{7}$$

2.1.2. FE models for shearing stiffnesses

Nordstrand et al. [7] employs a three-point bending test and FE model thereof to determine the shearing stiffnesses of sandwich panels. Incompressible sandwich panel theory is employed to assume that the resultant shear stress produced by the centrally-applied load is carried only by the core layer, and not by the facing sheets. Therefore, the vertical deflection, Δ, of the simply-supported sandwich panel is computed as,

$$\Delta = \frac{WL^3}{48bD_i} + \frac{WL}{4AG_{iz}} \tag{8}$$

where $i=x,y$, depending on the orientation of the specimen or, in the present case, the FE model geometry. Furthermore, L is the sample length, D_i is the flexural rigidity per unit length of the panel and AG_{iz} is the equivalent shear stiffness. The panel cross-sectional shearing area is $A = bh_f^2/(h_f - t_f)$, where b is the specimen width. Schematics of the FE model geometries of the three-point bending tests to compute the equivalent shearing stiffnesses are depicted in Fig. 3(a) and (b).

The model is evaluated for a variety of specimen lengths, L. Vertical deflection of the facing sheet opposite the force, W, is evaluated at a centrally located node of the sample for each run of the model. As per Nordstrand et al. [7], a plot of Δ/WL^3 against $1/L^2$ is generated. The y-intercept of the plot is $1/48bD_i$ while the slope is $1/4AG_{iz}$. Therefore, by simulation of the three-point bending test for a number of sample lengths, L, the appropriate equivalent shearing stiffness G_{iz} is determined.

2.2. Comparison of the undamped eigenfrequencies

A sandwich structure with the periodic cross-section of Fig. 1(a) and with the characteristics reported in Table 1 was considered. In this paper, all simulations were performed using the commercial FE software package COMSOL Multiphysics. Equivalent material properties were computed using the above methods and are provided in Table 2. The first 15 undamped eigenfrequencies of the structure were computed, first, using the

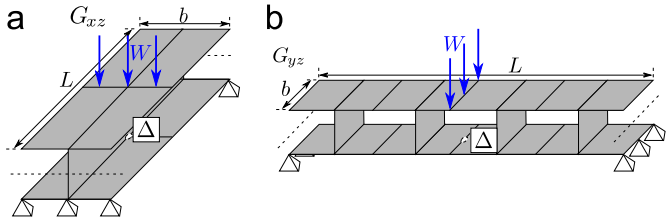

Fig. 3. (a) FE model to compute equivalent G_{xz} elasticity parameter of sandwich panel. (b) FE model to compute G_{yz}. Edges of the geometries are simply supported and a linear load, W, is applied to the specimen center.

Table 1
Elastic constants used in FE models.

Constants	Description	Value
a	Length of panel (m)	4.064
b	Width of panel (m)	4.064
$2p$	Period of sandwich panel core (m)	0.4064
h_f	Thickness of sandwich panel (m)	0.1016
E_c	Young's modulus of the core layer (GPa)	10.8
E_f	Young's modulus of the facing sheets (GPa)	2.10
t_c	Thickness of core layer (m)	0.0381
t_f	Thickness of facing sheet (m)	0.0127
ρ_c	Core density (kg m^{-3})	450
ρ_f	Facing sheet density (kg m^{-3})	760
ν_c	Poisson's ratio of the core layer	0.29
ν_f	Poisson's ratio of the facing sheet	0.24

Table 2
Computed equivalent elasticity parameters.

E_x (GPa)	E_y (GPa)	ν_x	ν_y	G_{xy} (MPa)	G_{yz} (MPa)	G_{xz} (MPa)	ρ_{eq} (kg m^{-3})
2.2	1.38	0.246	0.244	331.3	0.62	46.68	201.7

exact structure geometry in a full 3-D FE model discretized into triangular shell elements and, second, using an equivalent 2-D thick (Mindlin) plate analysis also using triangular elements. Meshing was not set for specific element size but was fine enough to include no fewer than 8 elements per model characteristic length, e.g., $2p$ in the model of Fig. 2(b), which assured the grid independence of the computational results. Boundary conditions were prescribed as follows. In the full 3-D FE model, the four vertical edges forming the corners of the structure were pinned. In the equivalent 2-D FE model, the four corners of the plate were fixed.

The first 15 undamped eigenfrequencies of the structures were computed by both models and are given in Table 3. For these lowest order modes, the average absolute deviation between methods is 2.0%. There is a significant difference in eigenfrequency computation for the third mode, resulting perhaps from the specific modeling of the boundary conditions. Ignoring this outlier, the average absolute deviation between models for the 15 lowest order eigenfrequencies is 1.4%. A comparison of several eigenmode shapes computed by the two methods is shown in Fig. 4. Even for the 13th mode, there is a clear consensus between the two models, indicating that the 2-D model of much reduced computational expense may be further employed with confidence. It is noted that the 3-D FE model used 70,000 shell elements while the 2-D FE model used only 10,000 elements when setting the maximum element size to be the same for each model.

Table 3
Comparison of first 15 eigenfrequencies (Hz) computed from full 3-D and equivalent 2-D FE models with percentage differences.

Mode number	Full 3-D model	Equivalent 2-D model
1	7.08	7.09 (+0.14%)
2	12.81	12.68 (−1.0%)
3	14.67	13.21 (−9.9%)
4	16.48	15.90 (−3.5%)
5	22.72	22.10 (−2.7%)
6	26.41	25.99 (−1.6%)
7	28.34	27.88 (−1.6%)
8	30.14	29.94 (−0.66%)
9	36.17	35.33 (−2.3%)
10	37.29	37.38 (+0.24%)
11	42.31	42.38 (+0.16%)
12	44.14	43.48 (−1.5%)
13	46.57	45.14 (−3.1%)
14	49.31	49.06 (−0.51%)
15	50.09	49.30 (−1.6%)

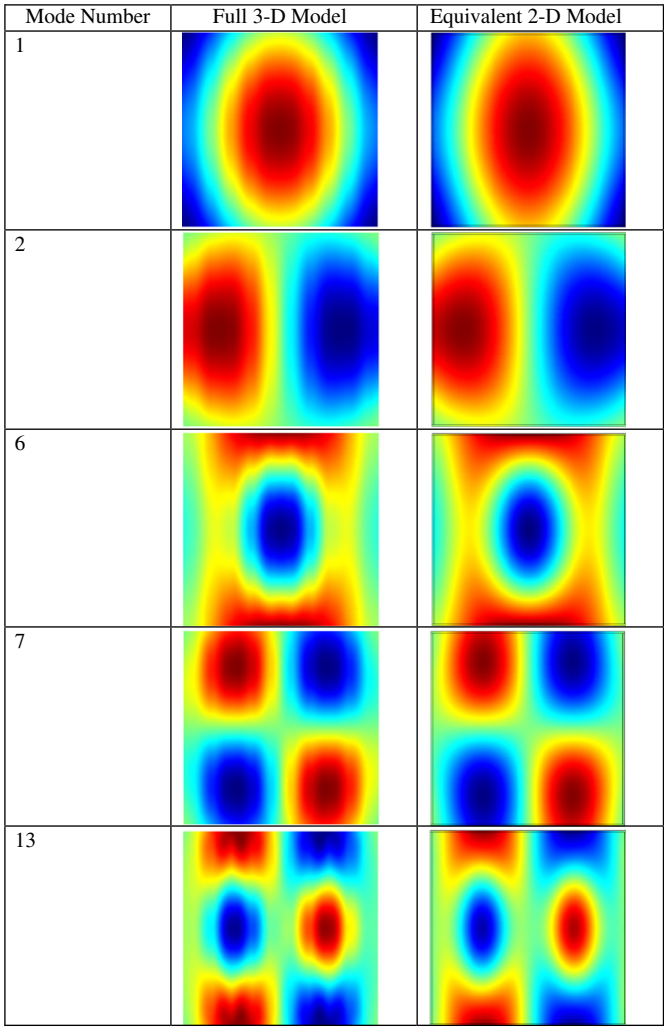

Fig. 4. Comparison of eigenmode shapes of low order sandwich panel vibration from full 3-D and equivalent 2-D FE models.

3. Introduction of punctual connections between the layers

3.1. Determination of the seven equivalent elastic constants

Oftentimes, sandwich structures are not bonded continuously but instead utilize a finite number of attachment locations. For instance, in the present building construction application of interest, the connections between the plates/boards and the studs are punctuated by nails. This section studies the influence of such punctuated connections on the computed equivalent elasticity parameters and, therefore, on the dynamic response.

The FE models from the previous sections were modified to include discrete connections between the facing panels and the core layer (e.g., studs). These connections represent nails in the structure having geometry as depicted in Fig. 5. The square nails have characteristic dimension, l_c, height, h_c, and are spaced d_c apart. Square-shaped connections were utilized due to the ease of constructing the FE mesh for each model revision. The joints were considered an isotropic material having a Young's modulus six orders of magnitude greater than the facing plates. This selection eliminates the possibility of local deformation in the joint itself as compared to the full sandwich structure.

3.2. Comparison of the undamped eigenfrequencies

Following each selection of connection distance d_c, the equivalent elastic constants of the sandwich structures were computed using the FE models described in Section 2. The exact sandwich panel geometry and material properties employed were those provided in Table 1. The punctuated element characteristic dimension was fixed at l_c=2 mm.

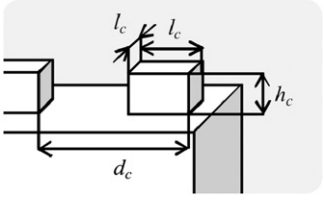

Fig. 5. Modeling of punctuated connection between facing sheets and core layer, facing sheet removed from image to visualize the connection geometry.

Table 4
Computed elastic constants as a function of d_c/L (% differences computed from $d_c/L=0$).

d_c/L	E_x (GPa)	E_y (GPa)	G_{xy} (MPa)	G_{xz} (MPa)	G_{yz} (MPa)	ν_x
0	2.199 (–)	1.377 (–)	331.3 (–)	46.68 (–)	0.6164 (–)	0.2458 (–)
0.019	1.800 (−8.1%)	1.331 (−3.34%)	291.1 (−12.1%)	18.05 (−61.3%)	0.2820 (−54.2%)	0.2393 (−2.64%)
0.036	1.810 (−17.7%)	1.330 (−3.41%)	281.8 (−14.9%)	9.350 (−79.9%)	0.2226 (−63.8%)	0.2403 (−2.24%)
0.066	1.827 (−16.9%)	1.332 (−3.27%)	286.5 (−13.5%)	4.872 (−89.5%)	0.1475 (−76.0%)	0.2402 (−2.28%)
0.090	1.833 (−16.6%)	1.332 (−3.27%)	272.8 (−17.6%)	3.164 (−93.2%)	0.1475 (−76.0%)	0.2407 (−2.07%)

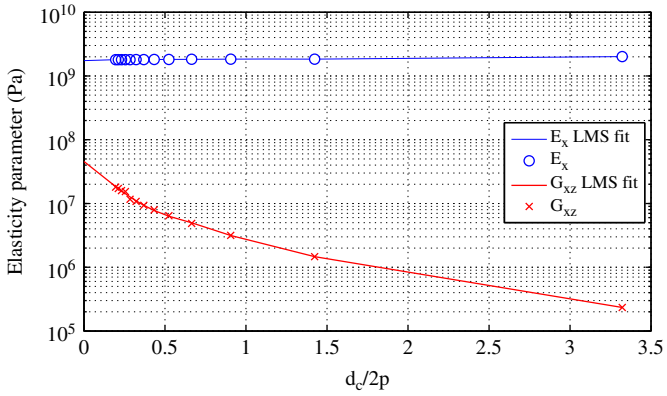

Fig. 6. Effect of punctuated connection spacing on the computation of equivalent bending stiffness, E_x, and transverse shearing stiffness, G_{xz}.

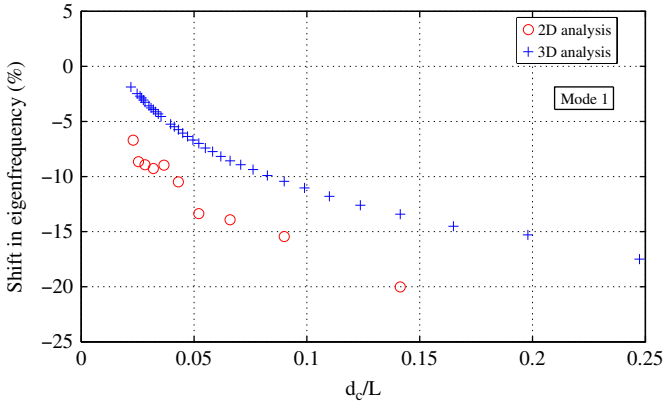

Fig. 7. Effect of punctuated connection spacing on the computation of the first undamped eigenfrequency.

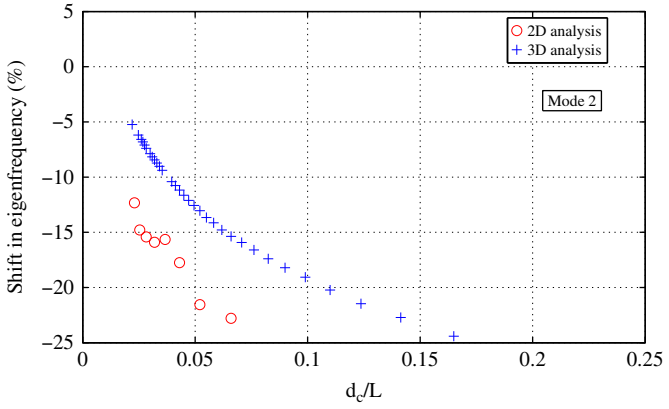

Fig. 8. Effect of punctuated connection spacing on the computation of the second undamped eigenfrequency.

Table 4 presents the change in the equivalent elasticity parameters as a function of the spacing between the punctual connections. As the spacing parameter d_c increases, the equivalent parameters are all observed to decrease from the continuous-contact case, $d_c=0$. This trend is intuitive since the core layer is the primary component strengthening the full sandwich structure; therefore, fewer connections between the facing panels and the core reduce the stiffness of the composite panel. Apart from the Poisson's ratio, ν_x, the parameters least affected by the discontinuous connection are the bending stiffnesses, E_x and E_y. Since the FE models utilize rigid elements at the ends for application of the necessary moments, the facing plates are not capable of significant sliding relative to the intermediary layer. Therefore, the bending stiffnesses are mostly a function of the sandwich panel geometry itself as opposed to the specific manner in which the sandwich structure is bonded together. More specifically, as demonstrated by Buannic et al. [10], the membrane and bending behaviors are driven mainly by the thickness of and the distance between the facing sheets, respectively. In contrast, the parameter most influenced by the decrease in contact between the facing panels and the sandwich core is G_{xz}. This is an intuitive result since shearing forces in the x direction attempt to tear or peel the facing plates away from the intermediary layer. Greater concentration of discrete connections bonding the three layers therefore yields a greater shearing stiffness G_{xz}.

Fig. 6 depicts the variation of the equivalent elastic constants E_x and G_{xz} as a function of the ratio $d_c/2p$. In the figure, the solid curves were determined from a linear least–squares fit to the computed elastic constants. It is readily apparent that G_{xz} is highly sensitive to changes in the punctuated connection spacing. A spacing equal to one period of the sandwich structure, i.e., $d_c/2p=1$, decreases the shearing stiffness by more than an order of magnitude whereas E_x is relatively unchanged.

Once the seven equivalent elastic constants were calculated for each case of joint spacing d_c, a new 2-D FE model was constructed of a panel having such anisotropic elasticity parameters. The panel dimensions were those provided in Table 1. Meanwhile, a full 3-D FE model of the actual sandwich structure was constructed using the known elastic constants for the facing sheets and core layer reported in Table 1. The resulting undamped eigenvalue problems were then solved for the first three modes of structure with boundary conditions described above.

Figs. 7–9 plot the results of the change in the lowest three undamped natural frequencies against the normalized connection spacing parameter, d_c/L. Data points marked by red circles denote results from the equivalent 2-D FE model whereas the blue crosses denote those from the full 3-D FE model. The percentage shift in the eigenfrequencies is computed using as a reference results from the full 3-D FE model with continuous connections between the layers, as reported in Table 2.

Each of the lowest three eigenfrequencies is observed to decrease rapidly as the distance between the connections increases. The frequencies calculated from the equivalent 2-D anisotropic panel are uniformly less than those of the full 3-D FE models in the presence of discontinuous contact between the

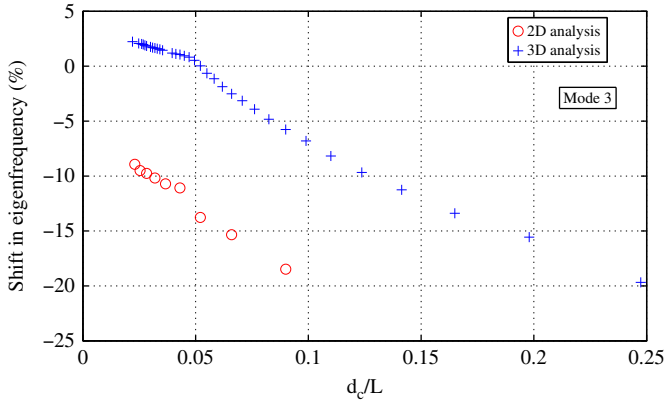

Fig. 9. Effect of punctuated connection spacing on the computation of the third undamped eigenfrequency.

facing plates and core layer. This may be attributed to the uniform reduction in the equivalent stiffnesses as d_c/L increased, indicated in Table 4. However, Table 3 showed that the eigenfrequency solutions converged as the spacing was decreased to the point of continuous contact, $d_c/L=0$. Thus, while an equivalent 2-D analysis may be appropriate for continuous connection between the layers, the inclusion of discrete connections amongst the layers quickly compromises the agreement between the equivalent 2-D and the full 3-D FE analyses. In the event of sparse connections between the core layer and facing sheets of a realistic structure, one must cautiously use the present approach for computing equivalent elasticity parameters.

4. Vibro-acoustic coupling

In many applications, sandwich structures are lined with fibrous or elastic porous materials to increase their acoustic- and thermal-insulation performance. For instance, in building construction, stud-framed walls often have their cavities filled with fiberglass wool. On the other hand, most numerical studies on the eigenproperties of sandwich structures assume in-vacuo conditions within the continuous medium and thus neglect the potential effects of a cavity–filling fluid or material on the structural response. Such effects are of interest and are investigated in this section.

4.1. Effect of a gas-filled cavity on the structural response

The undamped eigenproperties of sandwich structures, where cavities are filled in with various gases, were computed. The structures have the same geometry and boundary conditions as in the analysis of Section 2 but were fully enclosed, i.e., not being open-ended as shown in the FE model diagrams of Fig. 2. First, three structures are considered where each structure is made of one isotropic material with uniform thickness for facing sheets and core layer such that the total mass, M_s, of the structure is always equal to 205 kg. Table 5 reports the properties of the materials used to form the three structures. Second, one material (oak) is selected for which the thickness of the core and facing elements is changed so that the total mass of the structure is successively decreased to 20.5 kg and increased to 2050 kg. Seven gases are considered here, ranging from light (e.g., helium) to heavy (e.g., sulfur hexafluoride) gases. The properties of these gases and the total mass, M_g, of gases enclosed in the cavities are listed in Table 6. It is obvious that the parameters in this analysis are not intended to be representative of realistic building structures but were selected solely for the purpose of conducting a parameter study. The study is therefore more representative for such sandwich structures which may be far more susceptible to choice of the gas within the cavity. For example in the packaging of MEMS, gas-filled cavities plays a pivotal role in the damping of the devices heavily influencing the dynamics of the MEMS device in question [13,14].

Table 5
Properties of the materials used to form the three structures.

Material	E (GPa)	ρ (kg m^{-3})	ν	Thickness (mm)
Aluminum	70	2700	0.35	2
Oak	12	630	0.35	0.0857, 0.857, 8.57
Cork	0.1	250	0.15	21.6

Table 6
Properties of the gases used to fill in the cavities of the structures.

Gas	ρ (kg m^{-3})	c_f (m s^{-1})	Total mass (kg)
Helium	0.16	927	0.24
Neon	0.90	435	1.32
Air	1.21	343	1.78
Argon	1.45	323	2.13
Krypton	3.75	220	5.50
Xenon	5.89	169	8.65
Sulfur Hexafluoride	6.12	151	8.99

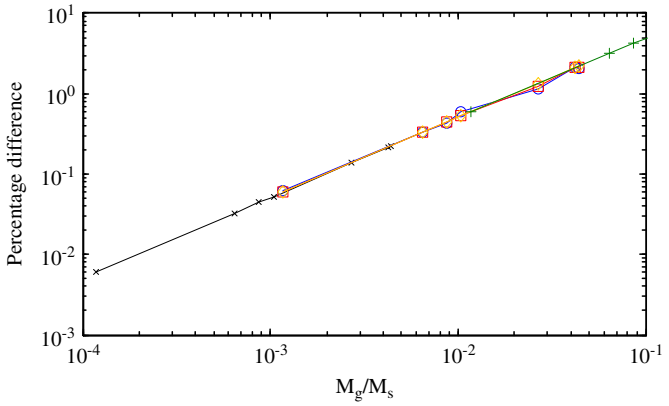

Fig. 10. Percentage difference between the first natural frequencies of the structures computed in vacuo and with gas in the cavities as a function of the ratio of the total mass of gas enclosed by the structure to the total mass of the structure. Aluminum (○), cork (◇), oak with total mass of 205 kg (□), oak with a total mass of 20.5 kg (×), and oak with total mass of 2050 kg (+).

For this fluid–structure interaction problem, interface boundary conditions were prescribed such that: (i) the facing sheets of the structure were loaded with a force per unit area equal to the pressure loading induced by the fluid and (ii) the particle acceleration of the fluid was equal to the structural acceleration of the facing sheets. Note that fluid–structure interaction was ignored at the interfaces between the fluid and core layer.

The first natural frequency of a structure filled with a gas is computed and compared to that of the structure in vacuo. Results are depicted in Fig. 10 for various structure-gas configurations. In the figure, all curves are nearly linear and superimpose. This result demonstrates that the logarithm of the change in the structural natural frequency that is induced by the presence of the gas in the cavities is linearly proportional to the logarithm of the total mass of gas added to the system and is independent of the elastic properties of the components forming the structure. Similar results (not plotted here) are observed for higher order modes. For all structures with a total mass of 205 kg considered in

the analysis, air induces a change in the first natural frequency that is less than 0.5%. Given the trend of the curves, a 10% percentage change in the first natural frequency would be expected if the structure was enclosing air and its total mass would be 9 kg.

These results indicate that the assumption of in-vacuo conditions when computing the equivalent elastic parameters of sandwich structures is seen to be a valid one, with the exception of extremely lightweight structures.

Fig. 11 depicts the first three modes of the aluminum structure with air enclosed in the cavities. In the first mode (also observed for the structure in vacuo), the structure deforms in a global fashion as one uniform continuum would. The second and third modes correspond to deformations of the facing sheets only (local behavior). These additional modes are not observed for in-vacuo conditions and thus are clearly induced by the presence of gas in the cavities and the geometry of the cavities themselves. The amplitudes of these local deformations are insignificant (smaller by at least one order of magnitude) compared to the global deformation observed in the first mode. The effect of these cavity-induced modes on the frequency response of the structure to a point-force excitation is described next.

4.2. Effect of a porous material on the structural response

The cavities of the aluminum structure described above are now filled with a porous elastic material. It was demonstrated that for this structure, the effect of air-filled cavities on the structural eigenproperties are insignificant. Therefore, the porous material is modeled as a structural element and the analysis collapses to the interaction between two structures with significantly different elastic properties. The properties of polyurethane foam are selected for this analysis [15]: Young's modulus $E=17\times10^5$ Pa, Poisson ratio $\nu=0.4$, loss factor $\eta=0.27$, and density $\rho=30\ \mathrm{kg\,m^{-3}}$. The ratio of the total mass of foam enclosed by the structure to the total mass of the structure is equal to 0.2. A loss factor $\eta=5\times10^{-3}$ is used to characterize structural damping in the aluminum structure at low frequencies.

For this structure–structure interaction problem, matching of the structural velocity was enforced at the interface of the elements forming the aluminum structure and the porous material. The frequency response function (FRF) is computed at the junction of a facing sheet and the core layer. The excitation is provided near a corner of the structure by a unit magnitude point force, from 1 to 100 Hz in steps of 1 Hz. Fig. 12 shows the geometry of the structure with the positions of the point force and virtual accelerometer. The FRF at the virtual accelerometer is shown in Fig. 13, for the case of the structure in vacuo (solid blue curve), with foam inside the cavities (dashed orange curve), and with air inside the cavities (crosses).

The FRF for the in-vacuo panel is highly resonant, characteristic of the lightly-damped aluminum sandwich structure. The inclusion of air in the cavities amplifies certain portions of the FRF since the additional gas acts in effect like a distributed spring between the two facing sheets, as shown by Pretlove [16] in the study of the vibration of a plate backed by a closed rectangular cavity. This is particularly evident at the 36 Hz resonance, which is amplified by approximately 2 dB. This spring-like resonant

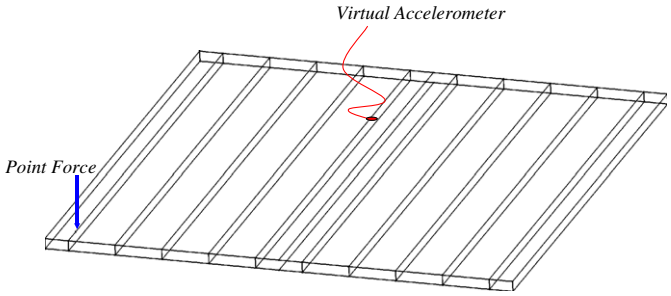

Fig. 12. Schematic description of the aluminum structure indicating the positions of the point-force excitation and virtual accelerometers.

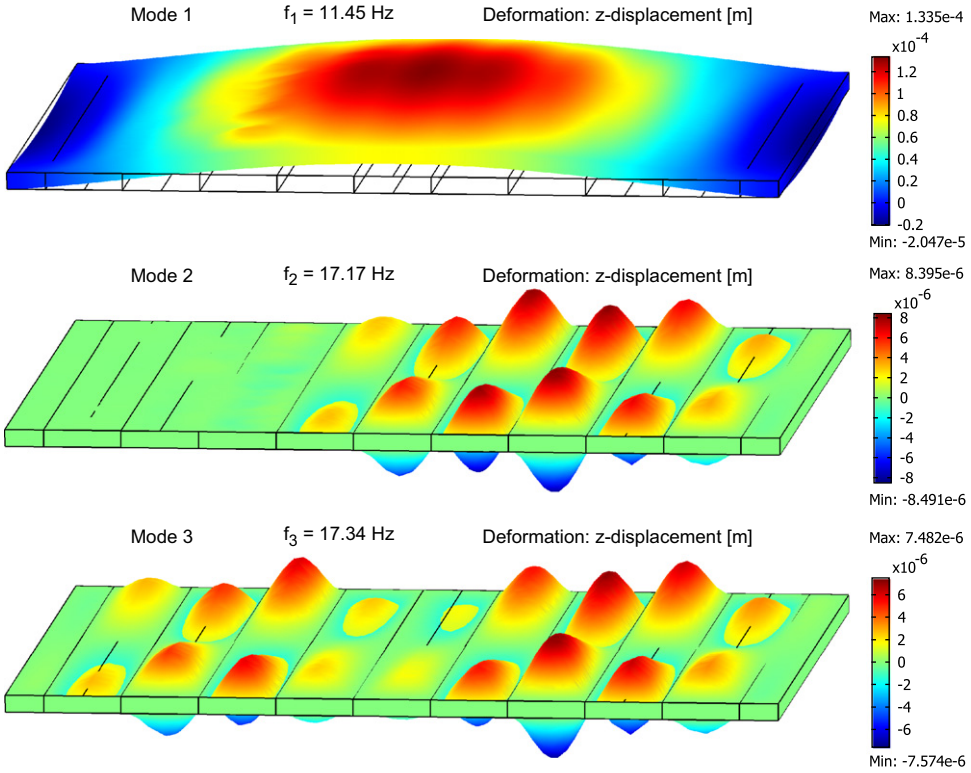

Fig. 11. First three modes of the aluminum structure with air enclosed in the cavities.

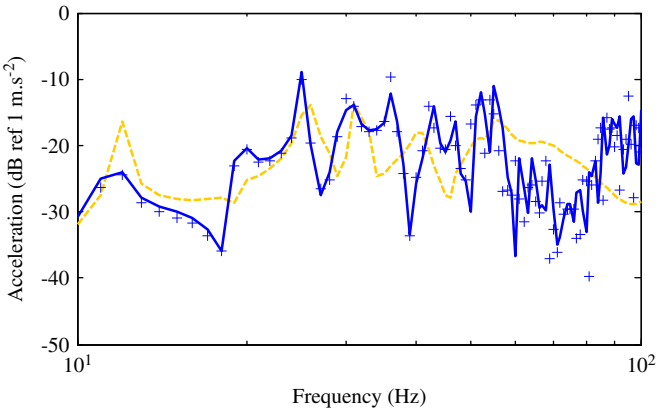

Fig. 13. Acceleration of the aluminum structure as a function of frequency due to a unit magnitude point force applied near a corner of the structure. In vacuo conditions (——), cavities filled in with polyurethane foam (– – –), and cavities filled in with air (+).

effect, which alters the magnitude of the FRF, is dependent on frequency and on the geometry of the individual cavity with which the gas interacts. However, apart from this minor and localized amplification, the presence of air in the cavities does not notably influence the overall FRF.

To a similar end, the presence of the foam within the cavities is also seen to alter the amplitude of several resonances. Most apparent is the amplification at the 12 Hz resonance. At higher frequencies, the tendency of the embedded foam is to dampen the structure through a combination of mass loading and viscous damping. Since the foam mass represents an increase of 20% to the total structural mass, this inclusion exerts substantial inertial resistance on the vibration of the sandwich structure and thereby dampens and lowers in frequency many of the higher resonances. In summary, the embedded foam material generally modifies the FRF response of the sandwich panel by damping the structural response. As most building construction scenarios would realistically include foam-like materials within the sandwich structure, the numerical approach described in this paper may compensate for this by prescribing a greater level of overall damping to the equivalent 2-D continuum.

5. Conclusions

A study of realistic features of sandwich panels, not otherwise accounted for in typical methods for computing the equivalent elasticity parameters, was carried out to determine the overall importance of these features on the applicability of the method. The analysis and convenient FE models to compute the equivalent elasticity parameters of sandwich structures were presented in detail. Computation of eigenfrequencies and eigenmodes for a sample sandwich panel was found to be in close agreement between the equivalent 2-D continuum and the full 3-D structure.

Realistic interfacial connections between the facing sheets and core layer were then considered. It was shown that such discrete connections generally reduce the various equivalent stiffness parameters of the sandwich panel, corresponding to a reduction in the computed eigenfrequencies with respect to the idealized sandwich structure having continuous connections between the facing sheets and core layer. As the discrete connections between core and facing materials were spaced further apart, eigenfrequencies of the equivalent 2-D panel were found to significantly deviate from solutions computed for the 3-D sandwich panel geometry, suggesting care must be taken when employing the equivalent 2-D method depending on the anticipated continuity between the facing and core layers of the studied structure.

For fully enclosed sandwich panels, the adequacy of in-vacuo assumptions in the approach for computing equivalent elasticity parameters was considered. It was shown that this assumption falters only when the structural mass is reduced to the point that the gas inside the sandwich panel cavities is substantial, ~10% of the panel mass. In conventional building construction, the cavities of sandwich structures are filled with acoustic and/or thermal insulation materials and this inclusion was considered. Elastic material within the panel cavities was found to act as both a distributed mass and stiffness affecting the host structure in a manner dependent on the embedded material properties and the cavity geometry. In general, the presence of an elastic material damped the structural response, which may be compensated for by modeling the equivalent 2-D continuum with greater overall damping.

Acknowledgments

This work was funded by the NASA Langley Research Center under Grant number NNL10AA05C, technical monitor Mr. Jacob Klos. This support is greatly appreciated. The authors wish to thank Dr. Patrice Cartraud (Ecole Centrale de Nantes, France) and Dr. Sylvie Pommier (Ecole Normale Supérieure de Cachan, France) for their valuable comments on the work presented.

References

[1] Milani G. A simple equilibrated homogenization model for the limit analysis of masonry structures. WSEAS Transactions on Applications Theoretical Mechanics 2007;2:119–25.
[2] Hans S, Boutin C. Dynamics of discrete framed structures: a unified homogenized description. Journal of Mechanics of Materials and Structures 2008;3:1709–39.
[3] Krstevska L, Tashkov L, Gocevski V, Garevski M. Experimental and analytical investigation of seismic stability of masonry walls at Beauharnois powerhouse. Bulletin of Earthquake Engineering 2010;8:421–50.
[4] Chong KP, Hartsock JA. Structural analysis and design of sandwich panels with cold-formed steel facings. Thin-Walled Structures 1993;16:199–218.
[5] Noor AK, Burton WS. Computational models for sandwich panels and shells. Applied Mechanics Reviews 1996;49:155–99.
[6] Libove C, Batdorf SB. A general small deflection theory for flat sandwich plates. NACA–TR–Report 899, USA, 1948.
[7] Nordstrand TN, Allen HG, Carlsson LA. Transverse shear stiffness of structural core sandwich. Composite Structures 1994;27:317–29.
[8] Lewinski T, Telega JJ. Plates, laminates and shells.Asymptotic Analysis and Homogenization. Singapore: World Scientific; 1999.
[9] Caillerie D. Thin elastic and periodic plates. Mathematical Methods in the Applied Sciences 1984;6:159–91.
[10] Buannic N, Cartraud P, Quesnel T. Homogenization of corrugated core sandwich panels. Composite Structures 2003;59:299–312.
[11] Burlayenko VN, Sadowski T. Analysis of structure performance of sandwich plates with foam-filled aluminum hexagonal honeycomb core. Computational Materials Science 2009;45:658–62.
[12] Cheng QH, Lee HP, Lu C. A numerical analysis approach for evaluating elastic constants of sandwich structures with carious cores. Composite Structures 2006;74:226–36.
[13] Choa SH. Reliability of vacuum packaged MEMS gyroscopes. Microelectronics Reliability 2005;45:361–9.
[14] Bao M, Yang H. Squeeze film air damping in MEMS. Sensors and Actuators A: Physical 2007;136:3–27.
[15] Bolton JS, Green ER. Normal incidence sound transmission through double-panel systems lined with relatively stiff, partially reticulated polyurethane foam. Applied Accoustics 1993;39:23–51.
[16] Pretlove AJ. Free vibrations of a rectangular panel backed by a closed rectangular cavity. Journal of Sound and Vibration 1965;2:197–209.